Check for updates

Development of self-compatible Chinese cabbage lines of Chiifu through marker-assisted selection

Lichun Chang†, Jianli Liang†, Xu Cai, Li Zhang, Yufang Li, Jian Wu* and Xiaowu Wang*

State Key Laboratory of Vegetable Biobreeding, Sino-Dutch Joint Laboratory of Horticultural Genomics, Institute of Vegetables and Flowers, Chinese Academy of Agricultural Sciences, Beijing, China

The continuously refined genome assembly of the Chinese cabbage accession Chiifu is widely recognized as the reference for *Brassica rapa*. However, the high self-incompatibility of Chiifu limits its broader utilization. In this study, we report the development of self-compatible Chiifu lines through a meticulous marker-assisted selection (MAS) strategy, involving the substitution of the Chiifu allele of *MLPK* (*M-locus protein kinase*) with that from the self-compatible Yellow Sarson (YS). A YS-based marker (SC-MLPK) was employed to screen 841 *B. rapa* accessions, confirming that all eight accessions with the *mlpk/mlpk* (*mm*) genotype exhibited self-compatibility. Additionally, we designed 131 High-Resolution Melting (HRM) markers evenly distributed across the *B. rapa* genome as genomic background selection (GBS) markers to facilitate the introgression of self-compatibility from YS into Chiifu along with SC-MLPK. Genome background screening revealed that the BC_3S_1 population had a proportion of the recurrent parent genome (PR) ranging from 93.9% to 98.5%. From this population, we identified self-compatible individuals exhibiting a high number of pollen tubes penetrating stigmas (NPT) (>25) and a maximum compatibility index (CI) value of 7.5. Furthermore, we selected two individuals demonstrating significant similarity to Chiifu in both genetic background and morphological appearance, alongside self-compatibility. These selected individuals were self-pollinated to generate two novel lines designated as SC-Chiifu Lines. The development of these self-compatible Chiifu lines, together with the SC-MLPK marker and the set of HRM markers, represents valuable tools for *B. rapa* genetics and breeding.

Introduction

Chinese cabbage (*Brassica rapa* ssp. *pekinensis*) accession Chiifu exhibits high self-incompatibility. Chiifu is the first *Brassica* accession to be sequenced and assembled as reference genome (Chiifu v1.5) (Wang et al., 2011). Advancements in sequencing technologies have led to the successive development of three updated genome assemblies (Chiifu v2.5, v3.0, and v4.0) (Cai et al., 2017; Zhang et al., 2018, 2023). The Chiifu genome serves as a prominent reference in the study of *Brassica* species, necessitating the mass selfed seeds. Additionally, the construction of a Chiifu mutant library assumes great significance, facilitating investigations into essential agronomic traits within *B. rapa*. However, the labor-intensive process of seed production in the highly self-incompatible Chiifu, reliant upon artificial pollination, poses challenges for its widespread application. In addressing this limitation, the development of a self-compatible Chiifu line with a high homozygosity of the genetic background (HGB) plays a crucial role in promoting genomic and genetic breeding studies of *Brassica* species.

The self-incompatibility (SI) in Chinese cabbage is regulated by a multi-allelic *S* locus, encompassing three genes associated with pollen-pistil recognition: *SRK* (*S-locus receptor kinase*), *SCR/SP11* (*S-locus cysteine-rich protein/S-locus protein 11*), and *SLG* (*S-locus glycoprotein*) (Yamamoto et al., 2023). The genetic set of alleles of these genes at the same *S* locus is designated as the '*S* haplotype' (Nasrallah and Nasrallah, 1993). Incompatible reactions occur when the pistil and pollen share the same *S* haplotype. Additionally, *ARC1* (*arm repeat-containing 1*), *THL1* (*thioredoxin-h-like-1*), *MLPK*, and *FER-Rac/Rop* signaling (*FERONIA receptor kinase homolog* or *Rac/Rop guanosine triphosphatase* signaling), not associated with the *S* locus, are involved in the pathways of the SI response (Stone et al., 1999; Cabrillac et al., 2001; Murase et al., 2004; Zhang et al., 2021).

Yellow Sarson (YS) (*B. rapa* ssp. *tricolaris*) carries a recessive mutation of the modifier (*m*) gene, eliminating the SI response in the stigma (Murase et al., 2004). The *M* gene, responsible for this trait, encodes a membrane-anchored protein kinase (MLPK). A SNP induces a specific amino acid substitution (Gly to Arg) at position 194 (G194R) (Murase et al., 2004). The dysfunctional G194R form of MLPK protein in *mm* plants can be restored through the transient expression of *MLPK*, thereby reinstating the ability of *mm* papilla cells to reject self-pollen (Murase et al., 2004). Two distinct forms of *MLPK*, *MLPK form 1* (*MLPKf1*) and *MLPK form 2* (*MLPKf2*), localize to the papilla cell membrane and directly interact with *SRK* to transduce SI signaling (Kakita et al., 2007). The Chiifu accession carries the S^{60} haplotype on chromosome A07 (Yamamoto et al., 2023), characterized by *MLPK*-dependent self-incompatibility (Ohata et al., 2023). However, the practical challenge of breeding self-compatible Chinese cabbage lines based on *MLPK* remains unresolved.

The fusion of genomics and breeding has accelerated the development of cultivars with enhanced traits (Dou et al., 2022; Liu et al., 2022; Cai et al., 2023; Li et al., 2023). Utilizing trait-specific markers in conjunction with genomic background analysis has proven to be a potent breeding strategy for overcoming SI.

Notably, in *Brassica oleracea*, the construction of a linkage map has facilitated the identification of major quantitative trait loci (QTLs) linked to self-compatibility (SC). Moreover, SC genes have been rapidly introduced by marker-assisted backcrossing (MABC) using self-compatibility-specific markers and 36 genomic background selection (GBS) markers (Xiao et al., 2019). The silencing of *SP11* gene within the *S* locus has led to the development of a self-compatible transgenic line in *B. rapa* (Jung et al., 2012). Leveraging the *S* locus in conjunction with 111 SSR markers distributed evenly on a physical map facilitated MABC, yielding a self-compatible line with a compatibility index (CI) of approximately 1.15 in Chinese cabbage (Zheng et al., 2022). Therefore, it is feasible to identify self-compatible accessions through screening *B. rapa* germplasm and subsequently develop self-compatible Chiifu lines via MABC.

HRM technology, capitalizing on the identification of distinct melting curves of PCR products, has emerged as a high throughput, accurate, and cost-effective tool for detecting genetic variations, including single nucleotide polymorphisms (SNPs), insertions or deletions (INDELs), and methylation (Herrmann et al., 2007; White et al., 2007; Distefano et al., 2012). In our previous study, we developed 148 INDEL markers for HRM genotyping in *B. rapa*, thereby expanding the repertoire of HRM markers in *B. rapa* (Chen et al., 2021). However, these HRM markers were solely designed based on a physical map as GBS markers. This result highlighted the advantage of HRM markers as genome background markers for marker-assisted selection.

This study aims to overcome the SI present in the *B. rapa* reference line Chiifu. We developed a functional-related marker (SC-MLPK) for *MLPK*. The accessions with *mlpk/mlpk* (*mm*) genotype identified by SC-MLPK across *B. rapa* subspecies proved all being self-compatible. Leveraging the constructed physical and genetic maps of *B. rapa*, we developed genetic background HRM markers evenly distributed across the genome. Through the combination of genotyping by the SC-MLPK marker and genetic background analysis for MABC, we successfully developed two self-compatible lines, designated as SC-Chiifu Lines by transferring the *mm* allele into Chiifu. Thus, this study provides valuable insights into the practical application of molecular markers for overcoming the SI in *B. rapa*.

Materials and methods

Plant materials

The *B. rapa* reference genome line Chiifu, characterized by a CI value < 1.0 at the anthesis stage, served as the receptor parent. Its *S*-haplotype is S^{60} (class II), as detailed in a recent study (Yamamoto et al., 2023). A Yellow Sarson line, R-o-18, exhibiting a CI value > 10, was employed as the donor parent. The initial cross involved mating the donor parent R-o-18 with the recurrent parent Chiifu, resulting in the generation of F_1 plants. Subsequent backcrossing was systematically performed with Chiifu, leading to the

development of backcross populations denoted as BC_1, BC_2, and BC_3. From the BC_3 generation, the BC_3-1, BC_3-6, and BC_3-7 plants with the *Mm* genotype and high proportion of recurrent parent genome (PR) were self-pollinated to yield BC_3S_1 populations. Individuals with both phenotypic and genetic background similarity to Chiifu while demonstrating self-compatibility were selected from the BC_3S_1 generation to be self-pollinated to produce self-compatible Chiifu lines (Figure 1). Additionally, this study included 841 accessions of *B. rapa* from our laboratory to identify individuals with *mm* genotypes. These accessions encompassed 207 Chinese cabbage, 189 Pak choi (ssp. *chinensis*), 150 Caixin (ssp. *parachinensis*), 119 European turnip (ssp. *rapa*), 76 Oil seeds (ssp. *oleifera*), 41 Yellow Sarson (ssp. *tricolaris*), 24 Japanese komatsuna (ssp. *perviridis*), 23 Japanese mizuna (ssp. *nipposinica*), and 12 Taicai (ssp. *chinensis* var. *tai-tsai*) (Cheng et al., 2016).

DNA extraction and whole-genome resequencing

Genomic DNA was extracted from all samples by the modified CTAB method (Mavrodiev et al., 2021). Plant materials selected for DNA library construction included R-o-18, BC_3-$1S_1$-6, BC_3-$6S_1$-15, and BC_3-$7S_1$-14. These samples were chosen to represent key stages

FIGURE 1
Overcoming high self-incompatibility in Chinese cabbage Chiifu through MABC. The numbers in square brackets indicate the number of plants. Gray arrows represent the process of constructing populations. Black arrows represent the selection by genotyping and phenotyping. The numbers in red, orange and cyan represent the number of markers with Chiifu, R-o-18 or heterozygote genotypes, respectively.

in the breeding program. For WGR, DNA libraries were prepared and subsequently sequenced on a BGISEQ-T7 platform employing paired-end 150 bp (PE150) reads. To ensure the production of high-quality data, the raw sequencing reads were filtered using the fastp software, adhering to default parameters (Chen et al., 2018).

Variant calls (SNPs/INDELs)

High-quality reads were aligned to the *B. rapa* Chiifu reference genome version 3.0 using Burrows-Wheeler-Alignment (BWA) software with the "mem" method (Li and Durbin, 2009; Zhang et al., 2018). PCR-duplicated reads were filtered out using Samtools software (Li et al., 2009). Variant datasets (SNPs/INDELs) were obtained by applying stringent filters to exclude variants with low quality or multi-allelic features (QUAL < 60, QD < 20, MQ < 30, FS > 13) using GATK software (McKenna et al., 2010; Chang et al., 2023). Additionally, heterozygous loci in the variant datasets of R-o-18 were excluded. Sequence variants of the *MLPK* gene between the reference genome Chiifu v3.0 and R-o-18 aligned reads were visualized using the Integrated Genome Viewer (IGV) software (Robinson et al., 2011). The analysis was conducted with an updated version of genome annotation (Chiifu v3.5) to ensure precision in interpreting the genomic variations (Zhang et al., 2022b).

MLPK-specific marker design and kompetitive allele-specific PCR genotyping

KASP genotyping was employed to discern specific SNPs associated with the *MLPK* gene. Prior to designing the *MLPK*-specific marker, an extensive investigation into SNPs affecting *MLPK* functionality was conducted. Initially, SNPs within *MLPK* were extracted from the SNP dataset of 524 *B. rapa* genomes, as reported in a previous study (Cai et al., 2021). Subsequently, the precise SNP responsible for the G194R mutation within *MLPK*, which has been reported by Murase et al. (2004), was identified. Utilizing this SNP information, an *MLPK*-specific marker was designed using Primer3 software (Untergasser et al., 2012). Furthermore, accessions carrying the *mm* genotype were identified from the SNP dataset of 524 *B. rapa* genomes, with one such accession serving as a positive control for subsequent KASP genotyping.

Amplification and allelic discrimination for the KASP marker were performed using the Scientific QuantStudio™ 12K Flex Real-Time PCR System (Thermo Fisher Scientific, USA). The KASP genotyping protocol followed the methodology outlined in a previous study (Zhang et al., 2022a). Details regarding the KASP reaction volume and thermal cycling conditions for SC-MLPK are provided in Supplementary Tables S1 and S2, respectively.

Assessment of CI values

The CI value was determined following a previously published protocol (Xiao et al., 2019). Approximately 20 flowers per
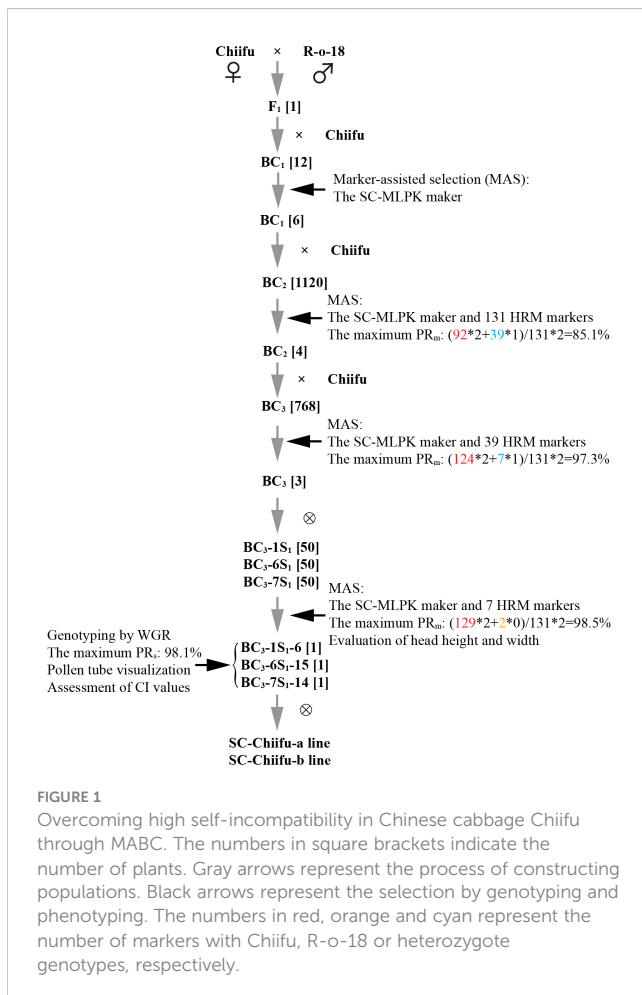
individual were manually self-pollinated one or two days after reaching full bloom. At the podding stage, CI was calculated using the formula: CI = number of seeds/number of pollinated flowers. Levels of SI, moderate self-compatibility (MSC), or SC were categorized as follows: SI (CI < 1); MSC ($1 \leq$ CI ≤ 4); SC (CI > 4). *B. rapa* accessions with the *mm* genotype, Chiifu, R-o-18, BC_3S_1 individuals with the *mm* genotype, were assessed of CI values. Additionally, from the BC_2 generation, plants with *Mm* genotypes were self-pollinated to generate BC_2S_1 populations. BC_2S_1 individuals with the *mm* genotype were assessed of CI values. All pollinations were conducted in the experimental greenhouse of IVF-CAAS, Beijing, China, at around 10:00 a.m. on sunny days.

Genome-wide HRM marker design and HRM genotyping

Genome-wide INDELs were selected from variant datasets derived between Chiifu and R-o-18. The Primer3 software was employed to design INDEL markers, utilizing 150 bp sequences flanking each INDEL locus (Untergasser et al., 2012; Chen et al., 2021). The designed INDEL markers produced amplicons ranging from 130 bp to 260 bp, with primer lengths between 18 bp and 23 bp. Melting temperature (Tm) predictions for each amplicon were carried out using the nearest-neighbor model (Breslauer et al., 1986; SantaLucia, 1998), setting parameters such as the concentration of sodium ions and reaction temperature to 1 M and 37 °C, respectively. ΔTm for each INDEL amplicon was predicted, and INDEL markers with a ΔTm greater than 0.5°C were retained as HRM markers.

To address the limitations of physical distance in reflecting genetic recombination rates, HRM markers were anchored to the constructed genetic linkage map in *B. rapa* based on their physical positions (Liu et al., 2016). Genome-wide HRM markers, evenly distributed across 10 chromosomes of *B. rapa*, were chosen for HRM genotyping, guided by both physical and genetic maps. Amplification and allelic discrimination for HRM genotyping were performed following a previously reported method (Chen et al., 2021).

Genetic background analysis using WGR data and HRM markers

WGR data of representative individuals (BC_3-$1S_1$-6, BC_3-$6S_1$-15, BC_3-$7S_1$-14, and R-o-18) were mapped to assembly of Chiifu. Firstly, whole-genome SNP datasets were generated using the Variant Calls method. Loci with missing genotypes were filtered out from the SNP datasets. Genotypes obtained from the SNP datasets were anchored to the physical map based on their respective physical positions. Graphical genotyping analysis was conducted using our Python script available at https://github.com/clc-CAAS/Genetic_map_construction.

PR was calculated after genotyping using the formula: PR = (Recurrent parent allele count * 2 + Heterozygous allele count * 1 + Donor parent allele count * 0)/Total allele count * 2. HGB was

calculated after genotyping using the formula: HGB = Homozygous allele count/Total allele count. To distinguish genotyping by HRM markers and WGR data, PR and HGB were designated as PR_m and HGB_m, respectively, when calculated after genotyping by HRM markers, and as PR_s and HGB_s, respectively, when calculated after genotyping by WGR data.
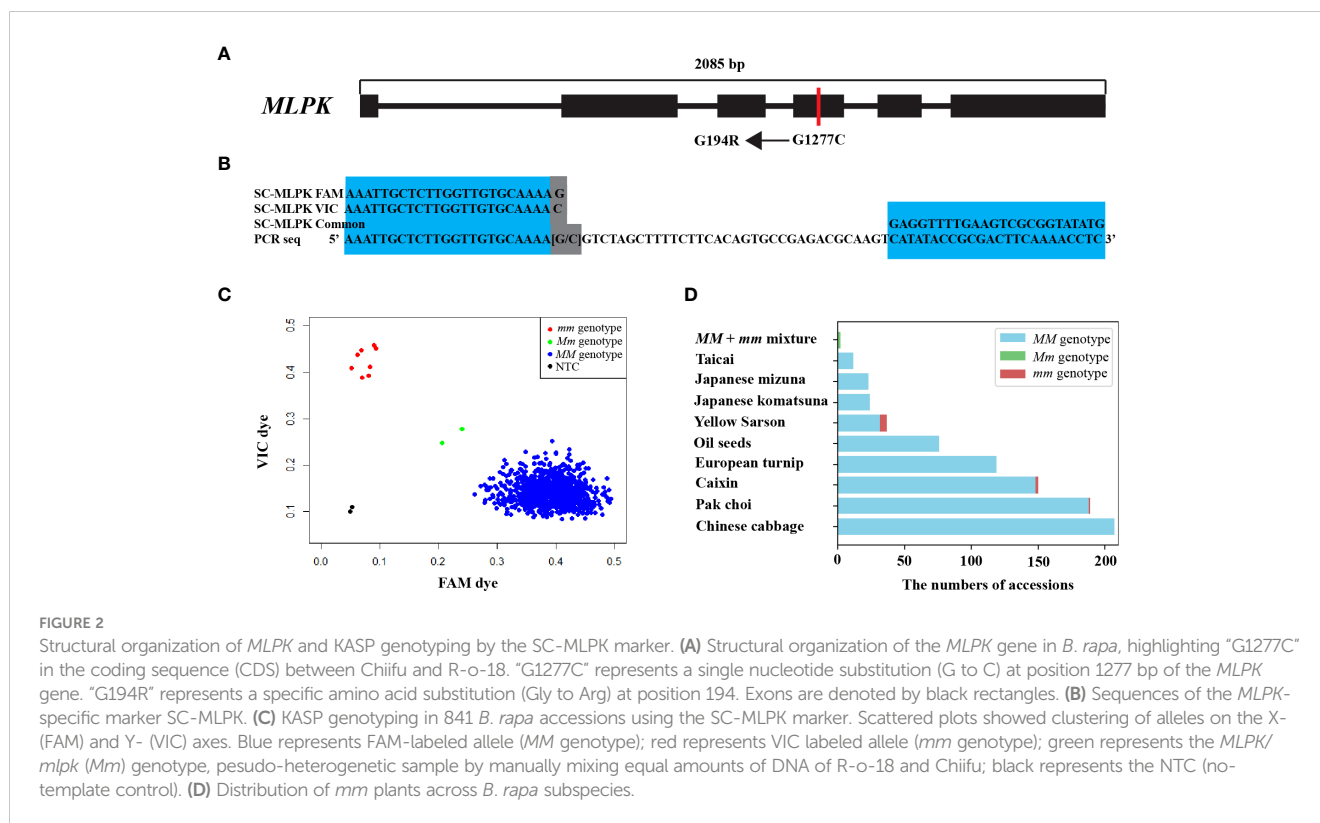
Pollen tube visualization

Chinese cabbage flowers from Chiifu, R-o-18, BC_3-$1S_1$-6, BC_3-$6S_1$-15, and BC_3-$7S_1$-14 were manually pollinated with a consistent amount of self-pollen grains one or two days after reaching full bloom. Ten flowers were selected for each individual. After 6 hours, stigmas were cut 2 mm away from the stigmatic surface for aniline blue staining to visualize pollen tubes following a published approach (Zhang et al., 2021). Stigmas were fixed in Canoy's fixative (methanol: acetic acid = 3:1), softened in 10 M NaOH, and stained with 0.1% aniline blue. Pollen tubes were visualized under UV fluorescence using a Leica MSV269 Stereo Microscope, and images were captured with a Leica DFC450 digital camera. SI, MSC or SC was assessed by the number of pollen tubes penetrating stigmas (NPT). The levels of SI, MSC or SC were classified as follows: SI (NPT < 10), MSC ($10 \leq$ NPT ≤ 25), SC (NPT > 25).

Results

Self-compatibility of *mm* plants across 841 *B. rapa* accessions

To identify the SNP responsible for inducing G194R within *MLPK*, we examined SNP datasets from 524 *B. rapa* genomes (Cai et al., 2021). We identified a total of 26 SNPs within *MLPK* (Supplementary Table S3). A single nucleotide substitution (G to C) at position 1277 bp (G1277C) in the fourth exon of *MLPK* was found to induce the G194R substitution (Figure 2A; Supplementary Table S4). This G1277C mutation was present in only five out of 524 *B. rapa* genomes, while the *MLPK/MLPK* (*MM*) genotype observed in 509 genomes and missing genotype data in 10 genomes. Additionally, sequence variants of *MLPK* between Chiifu and R-o-18 were visualized, as illustrated in Supplementary Figure S1. We developed a specific KASP marker named SC-MLPK based on the G1277C mutation (Figure 2B; Supplementary Table S5). We optimized the thermal cycling conditions of SC-MLPK for KASP genotyping, determining that 32 cycles after touchdown in the PCR program were superior to the native 26 cycles (Supplementary Figure S2; Supplementary Table S2).

To identity accessions with *mm* genotypes, we genotyped 841 *B. rapa* accessions by SC-MLPK marker assay. Eight accessions with the *mm* genotype were identified, including five yellow sarson, one pak choi, two caixin. Notably, the *mm* genotype was not detected in any accessions of Chinese cabbage (Figures 2C, D). To further confirm the self-compatibility of the *mm* plants, we accessed CI values for these eight accessions (Table 1), revealing CI values ranged from 4.25 to 16.3 among them. These results demonstrated

FIGURE 2

Structural organization of *MLPK* and KASP genotyping by the SC-MLPK marker. **(A)** Structural organization of the *MLPK* gene in *B. rapa*, highlighting "G1277C" in the coding sequence (CDS) between Chiifu and R-o-18. "G1277C" represents a single nucleotide substitution (G to C) at position 1277 bp of the *MLPK* gene. "G194R" represents a specific amino acid substitution (Gly to Arg) at position 194. Exons are denoted by black rectangles. **(B)** Sequences of the *MLPK*-specific marker SC-MLPK. **(C)** KASP genotyping in 841 *B. rapa* accessions using the SC-MLPK marker. Scattered plots showed clustering of alleles on the X- (FAM) and Y- (VIC) axes. Blue represents FAM-labeled allele (*MM* genotype); red represents VIC labeled allele (*mm* genotype); green represents the *MLPK/mlpk* (*Mm*) genotype, pesudo-heterogenetic sample by manually mixing equal amounts of DNA of R-o-18 and Chiifu; black represents the NTC (no-template control). **(D)** Distribution of *mm* plants across *B. rapa* subspecies.

that all of the eight accessions with *mm* genotypes were self-compatible. Thus, the *mm* genotype emerged as a potential factor for overcoming self-incompatibility in *B. rapa*.

Development of 131 HRM markers evenly distributed across 10 chromosomes

To facilitate the introgression of *mm* allele into Chiifu through MABC, we developed HRM markers which discriminate genome backgrounds between Chiifu and R-o-18. By aligning 10 Gb WGR data of R-o-18 to the reference genome Chiifu v3.0, a total of 665,095 INDELs were identified. Among these, 188,289 INDELs meeting stringent criteria of homozygosity and a length of ≥ 3 bp

were selected for marker design. Furthermore, 131 co-dominant HRM markers (Supplementary Table S6) evenly distributed across 10 chromosomes of the *B. rapa* (Table 2), were successfully developed for MABC. The ΔTm (melting temperature difference) values of INDEL amplicons between Chiifu and R-o-18 ranged from 0.8 °C to 2 °C for these HRM markers. The number of HRM markers ranged from 10 on chromosomes A07 and A08 to 17 on chromosome A03. The average genome-wide density of HRM markers was 2.28 Mb, ranging from 1.48 Mb on A10 to 3.01 Mb on A09. Furthermore, the average genetic interval across the genome was 7.29 cM, with a range from 5.15 cM on A10 to 9.04 cM on A07 (Table 2). The HRM genotyping for a representative HRM marker on each chromosome is depicted in Supplementary Figure S3. The 131 evenly distributed HRM markers across 10

TABLE 1 The CI value in *mm* plants.

Accessions	Genotype	Type	No. pollinated flowers	No. seed	CI value
611TWXBC	*mm*	Pak choi	20	200	10
6TCX	*mm*	Caixin	20	120	6
T42CX	*mm*	Caixin	20	200	10
Dys 1	*mm*	YS	20	85	4.25
L33	*mm*	YS	20	326	16.3
RARS	*mm*	YS	20	135	6.75
CGN06840	*mm*	YS	20	197	9.85
R-o-18	*mm*	YS	20	230	11.5
Chiifu	*MM*	Chinese cabbage	20	2	0.1

TABLE 2 Total number of HRM markers designed for each *B. rapa* chromosome.

Chromosome	Physical length (bp)	Genetical distance (cM)	No. markers	Average density[1] (Mb)	Average density[2] (cM)	Max gap (cM)
A01	29595527	106.84	13	2.28	8.22	13.37
A02	31442979	98.25	12	2.62	8.19	12.31
A03	38154160	111.76	17	2.24	6.57	11.18
A04	21928416	71.58	13	1.69	5.51	8.5
A05	28493056	108.5	14	2.04	7.75	15.62
A06	29167992	98.83	13	2.24	7.6	11.49
A07	28928902	90.36	10	2.89	9.04	13.16
A08	22981702	71.88	10	2.3	7.19	12.43
A09	45156810	115.21	15	3.01	7.68	12.71
A10	20725698	72.11	14	1.48	5.15	9.7

[1]: The average density of HRM markers is calculated based on physical length. [2]: The average density of HRM markers is calculated based on genetic distance.

chromosomes were used for further MABC of *mm* allele introgression from R-o-18 into Chiifu.

Successful introgression of *mm* allele from R-o-18 into Chiifu

To facilitate the selection of individuals harboring the *Mm* genotype in successive backcrossing populations, the KASP assay for the SC-MLPK marker was applied to the BC_1, BC_2, and BC_3 populations. The distribution of individuals harboring the *Mm* genotype in each backcrossing population was as follows: BC_1 (6/12), BC_2 (n=534/1120), and BC_3 (n=390/768). An extensive population comprising 1120 individuals was utilized in the BC_2 population to expedite the selection process for plants with the *Mm* genotype and a high PR_m. The segregation ratio of *MM*: *Mm* in each backcrossing population aligned with the anticipated Mendelian ratio of 1: 1 ($P > 0.05$).

To streamline the genetic background analysis in the extensive BC_2 population, a two-step MAS strategy was implemented for individuals with the *Mm* genotype. In the first step, three HRM markers on chromosomes A01, A02, and A09 were used for preliminary selection (Supplementary Figures S4A-D). Subsequently, a total of 96 individuals selected from the first round screening were upon the second round selection using the left 128 HRM markers. Based on the result from assays by SC-MLPK and 131 HRM markers, the maximum PR_m in the BC_2 population was determined to be 85.1%. For background analysis of individuals with the *Mm* genotype in the BC_3 population, 39 markers with heterozygous genotypes from the BC_2 population were employed. The highest PR_m was 97.3% among the BC_3 population (Supplementary Figure S4D). These results elucidated that the genetic background of each backcrossing population progressively approached to that of Chiifu.

Three BC_3 individuals with *Mm* genotypes as well as high PR_m, including BC_3-1 (PR_m = 97.3%), BC_3-6 (PR_m = 95.1%), and BC_3-7 (PR_m = 94.7%), were retained for self-pollination to generate BC_3S_1

populations. From each BC_3S_1 population, ten *mm* genotype plants were selected to be genotyped using background HRM markers (Figure 3A). Genotyping revealed that PR_m for the BC_3S_1 population ranged from 93.9% to 98.5%. Three *mm* individuals with high PR_m and high HGB_m, namely BC_3-$1S_1$-6, BC_3-$6S_1$-15, and BC_3-$7S_1$-14, were retained from BC_3S_1 population. Genotyping indicated that the PR_m of BC_3-$1S_1$-6, BC_3-$6S_1$-15, and BC_3-$7S_1$-14 was 98.5%, 96.6%, and 95.8%, respectively. The HGB_m of BC_3-$1S_1$-6, BC_3-$6S_1$-15, and BC_3-$7S_1$-14 was 100%, 96.2%, and 99.2%, respectively.

To further confirm the high similarity of genetic backgrounds between the three BC_3S_1 individuals to that of Chiifu, we conducted WGR for them. Genome-wide SNPs were extracted from aligned reads, utilizing the *B. rapa* genome Chiifu v3.0 as a reference. Loci with missing genotypes for each sample were filtered, and SNPs with homozygous genotypes in R-o-18 were retained, resulting in the identification of 1.6 million SNPs spanning chromosomes A01 to A10. These SNPs were anchored to both physical and genetic maps (Figures 3B-D). Based on the SNPs, boundaries of introgressed segments were delineated in BC_3-$1S_1$-6, BC_3-$6S_1$-15, and BC_3-$7S_1$-14 (Supplementary Table S7). Genotyping revealed that the PR_s of BC_3-$1S_1$-6, BC_3-$6S_1$-15, and BC_3-$7S_1$-14 was 98.1%, 92.6%, and 88.5%, respectively. The HGB_s of BC_3-$1S_1$-6, BC_3-$6S_1$-15, and BC_3-$7S_1$-14 was 99.6%, 97%, and 96%, respectively (Table 3). The individual plant (BC_3-$1S_1$-6) with the highest PR_s of 98.1% in the BC_3S_1 population displayed a near-identical match with the recurrent parent Chiifu genotype, except for a specific region (approximately 5.2 Mb, from 12059865 to 17244940) of the *MLPK* gene linkage on chromosome A03 retaining the donor parent R-o-18 genotype (Figure 3B). This result indicated successful introgression of *mm* allele from R-o-18 into Chiifu.

Novel self-compatible Chiifu lines

To evaluate the phenotypic traits of individual plants within the BC_3-$1S_1$, BC_3-$6S_1$, and BC_3-$7S_1$ populations relative to Chiifu, we conducted a detailed analysis encompassing agronomic traits,
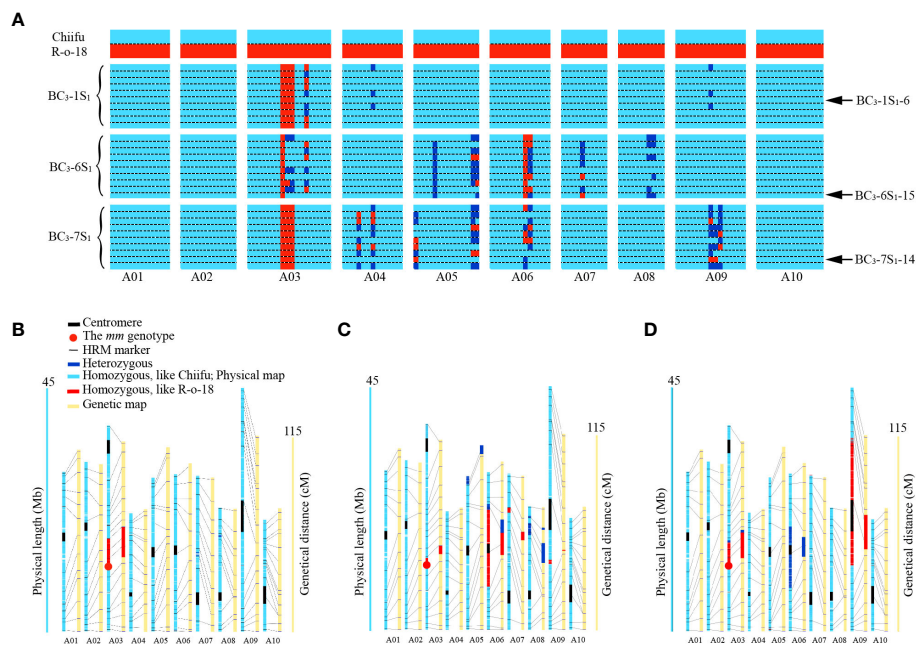
FIGURE 3
Genetic background analysis using markers and WGR. **(A)** Graphical genotyping based on polymorphism for SC-MLPK and 131 HRM markers. The vertical axis represents parental materials and ten introgression individuals of each BC_3S_1 population, while the horizontal axis represents SC-MLPK and 131 HRM markers (totaling 132 markers). Introgression individuals are grouped by different BC_3S_1 populations. The markers were organized according to their physical positions on the chromosomes. Arrow represents the selected individuals from each BC_3S_1 population. **(B-D)** Genotypes, determined by WGR, anchored to physical and genetic maps in BC_3-1S_1-6, BC_3-6S_1-15 and BC_3-7S_1-14, respectively. The yellow columns represent the genetic linkage groups corresponding to each chromosome. The centromere region is delineated by the black box. The red dot represents the mm genotype. Light blue segment indicated the homozygous genotype identical to Chiifu, red segment denoted the homozygous genotype identical to R-o-18, and navy blue segment represented the heterozygous genotype.

pollen tube visualization, and assessment of CI value (Figure 4). For agronomic trait analysis, 10 plants with mm genotype were selected from each BC_3S_1 population. Before leafy heads were ready for harvest, head height and width were evaluated and compared with Chiifu (Table 4). The head height and width ranged from 23.5 to 25.1 cm and 10.7 to 13.0 cm, respectively. Notably, both the average head height and width in BC_3-6S_1 population were not significantly different from those of Chiifu. In each BC_3S_1 population, all individuals exhibited heading, hairy, and crinkle traits similar to Chiifu, while the R-o-18 line displayed non-heading, hairless, and smooth traits. Three individuals including BC_3-6S_1-15, BC_3-1S_1-6, and BC_3-7S_1-14 exhibiting both genotypic and phenotypic similarity to Chiifu were selected from each BC_3S_1 population (Figures 4A-C; Supplementary Figure S5).

TABLE 3 PR and HGB in three selected individuals.

Individual	Genotype	PR_m (%)	HGB_m (%)	PR_s (%)	HGB_s (%)
BC_3-1S_1-6	mm	98.5	100	98.1	99.6
BC_3-6S_1-15	mm	96.6	96.2	92.6	97
BC_3-7S_1-14	mm	95.8	99.2	88.5	96
R-o-18	mm	0	100	0	100
Chiifu	MM	100	100	100	100

Upon flowering, BC_3-6S_1-15, BC_3-1S_1-6, and BC_3-7S_1-14, together with Chiifu, R-o-18, were investigated for pollen tube elongation and CI. Fluorescence microscopy revealed that R-o-18, BC_3-6S_1-15, and BC_3-7S_1-14 plants had more than 25 pollen tubes, whereas no pollen tubes were observed in BC_3-1S_1-6 and Chiifu (Figures 4D-F; Supplementary Figure S6). During the seed-filling stage, seed setting was evaluated (Figures 4G-I). Notably, BC_3-6S_1-15 and BC_3-7S_1-14 plants exhibited significant SC, achieving CI values of 7.5 and 7.1, respectively. In contrast, BC_3-1S_1-6 exhibited SI with a CI of 0.1, similar to that of Chiifu (CI = 0.1). Consequently, the two newly developed plants (BC_3-6S_1-15, BC_3-7S_1-14), which exhibited phenotypic and genetic similarities to Chiifu while demonstrating SC, were self-pollinated to generate two novel lines designated as SC-Chiifu Lines (SC-Chiifu-a, SC-Chiifu-b, respectively). The CI values of the SC-Chiifu Lines compared to the CI value of Chiifu (CI = 0.1) increased tenfold. However, the CI values of the SC-Chiifu Lines remained lower than that observed for R-o-18 (CI = 12). These results highlight the successful transfer of self-compatibility from R-o-18 into Chiifu, leading to the development of two novel SC-Chiifu Lines.

Segregation of SC in mm plants

In the BC_2S_1 population, 63 individuals with the mm genotype were selected for the assessment of CI values. The CI values varied significantly among these individuals, spanning from 0.2 to 13
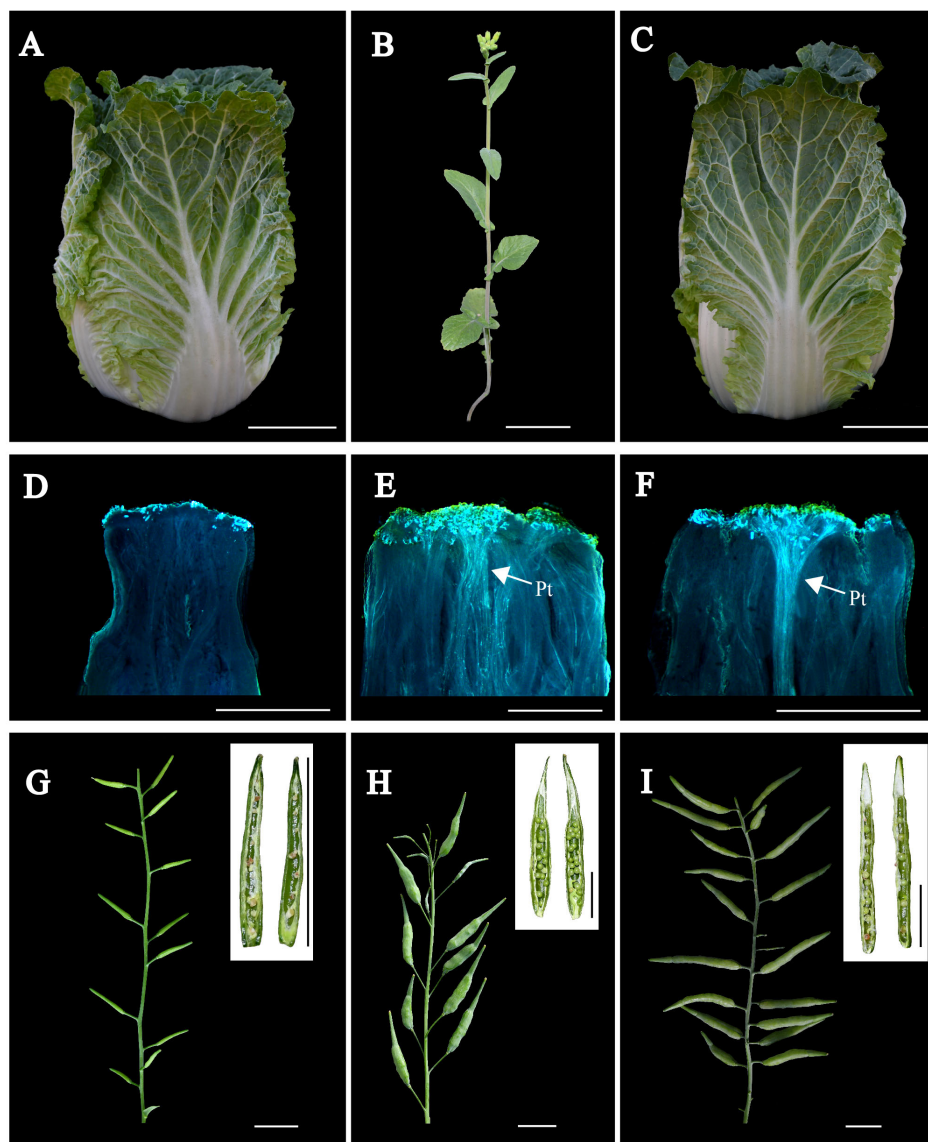
FIGURE 4

Comprehensive assessment of field and reproductive performance in Chiifu, R-o-18 and BC$_3$-6S$_1$-15 individual plants. **(A–C)** Field performance comparison of Chiifu, R-o-18, and BC$_3$-6S$_1$-15 plants. Scale bars in **(A–C)**, 5 cm. **(D–F)** Fluorescence microscopic images depicting pollen tube germination at the stigmas of Chiifu, R-o-18, and BC$_3$-6S$_1$-15 individual plants, with "Pt" indicating the pollen tubes. Scale bars in **(D–F)**, 1 mm. **(G-I)** Seed setting of Chiifu, R-o-18, and BC$_3$-6S$_1$-15 individual plants. Scale bars in **(G–I)**, 2 cm.

(Supplementary Table S8). Subsequent CI analysis delineated 29 individuals exhibiting SC (CI > 4), 22 individuals displaying MSC (1 ≤ CI ≤ 4), and 12 individuals manifesting SI (CI < 1). This observation indicated a pronounced segregation of SC within the *mm* plants of the BC$_2$S$_1$ population.

Furthermore, variations in SC were also observed among the three selected individuals (BC$_3$-6S$_1$-15, BC$_3$-7S$_1$-14, and BC$_3$-1S$_1$-6) with the *mm* genotype. Given that all three plants in the BC$_3$S$_1$ population possessed the same *mm* genotype and similar genetic backgrounds, the observed segregation suggested the involvement of gene(s) beyond the *MLPK* locus in influencing self-compatibility in *B. rapa*. We postulated that the gene(s) responsible being located at the segments shared by BC$_3$-6S$_1$-15 and BC$_3$-7S$_1$-14 individuals

are distinct from those in BC$_3$-1S$_1$-6. We examined *S* haplotypes in BC$_3$-1S$_1$-6, BC$_3$-6S$_1$-15, BC$_3$-7S$_1$-14, Chiifu and R-o-18 using *S*-specific primers (Oikawa et al., 2011). We found that BC$_3$-1S$_1$-6, BC$_3$-6S$_1$-15, and BC$_3$-7S$_1$-14, along with Chiifu, had S^{60} homozygotes, while R-o-18 exhibited an S^{54} homozygote. There was no correlation between CI value and *S* haplotype in BC$_3$-1S$_1$-6, BC$_3$-6S$_1$-15 and BC$_3$-7S$_1$-14. Based on our analysis on the introgressed segment boundaries in the three selected individuals, we identified four such segments (Figure 5). Specifically, four shared segments were located on chromosomes A03 (approximately 0.8 Mb, from 16451403 to 17244940), A06 (approximately 11.3 Mb, from 8101576 to 19449508), A07 (approximately 0.8 Mb, from 14002870 to 14798378), and A09 (approximately 0.7 Mb, from

TABLE 4   Analysis of agronomic traits in three BC$_3$S$_1$ populations.

	Line/population (Average $\pm$ SD)				
	BC$_3$-1S$_1$ (n=10)	BC$_3$-6S$_1$ (n=10)	BC$_3$-7S$_1$ (n=10)	Chiifu (n=10)	R-o-18 (n=10)
Head height (cm)	24.20 $\pm$ 1.64 ns	23.50 $\pm$ 1.36 ns	25.10 $\pm$ 0.79 *	23.70 $\pm$ 1.37	–
Head width (cm)	10.65 $\pm$ 1.13 *	11.35 $\pm$ 1.06 ns	13.00 $\pm$ 1.21 *	11.75 $\pm$ 0.49	–
Leaf head	Heading (100%)	Heading (100%)	Heading (100%)	Heading (100%)	Non-heading (100%)
Leaf hair	Hairy (100%)	Hairy (100%)	Hairy (100%)	Hairy (100%)	Hairless (100%)
Leaf crinkle	Crinkle (100%)	Crinkle (100%)	Crinkle (100%)	Crinkle (100%)	Smooth (100%)

A two-tailed t test was used to calculate significance between Chiifu line and each BC$_3$S$_1$ population. ns not significant; *$p<0.05$.

12255709 to 12997755). These findings suggested that these shared segments emerged as candidate segments potentially influencing SC.

Discussion

The production of self-pollinated seeds is difficult for Chiifu due to its high self-incompatibility, hampering it being widely used in genetic studies although the reference genome assemblies have been continuously updated. The small bud size of Chiifu adds to the complexity, making it challenging to manually open for self-pollination attempts. Despite efforts to self-pollinate during the bud stage, success rates are often low due to its small bud size and high self-incompatibility. Furthermore, the combination of high self-incompatibility and strong crossing compatibility exacerbates the issue by frequently leading to presence of contaminated hybrid seeds in the limited seed yield obtained from self-pollination attempts. In this study, we addressed the self-incompatibility issue in Chiifu by introducing the *mm* allele into this line. Through this genetic modification, we successfully developed two SC-Chiifu lines that not only retained genetic backgrounds closely resembling Chiifu but also exhibited self-compatibility phenotypes. The development of these SC-Chiifu lines enabled efficient seed setting without the need for manual pollination. This not only alleviates the challenges associated with self-pollination but also mitigates the risk of cross-pollen contamination.

Genetic background analysis within the SC-Chiifu Lines revealed that approximately 90% of the genetic segments originate from the recurrent parent, Chiifu, with the remaining 10% comprising exogenetic segments from the donor parent, R-o-18. Through the utilization of WGR data, we precisely delineated the boundaries of these exogenetic segments. This delineation offers valuable insights for future research endeavors involving the SC-Chiifu Lines. If the SC-Chiifu Lines are employed for updating the Chiifu genome, it is imperative to purify these exogenetic segments through targeted selection. Alternatively, for functional gene research, it may be feasible to disregard these exogenetic segments if they do not significantly impact the traits of interest, such as heading and leaf development. The SC-Chiifu Lines represent crucial plant materials for various applications, including the construction of a Chiifu mutant library and conducting Chiifu-based transgenic experiments. These lines are particularly valuable for breeding self-compatible heading Chinese cabbage, serving as ideal donor parents to provide self-compatibility and heading traits. In the study of self-compatibility mechanisms, both self-compatible SC-Chiifu lines and the self-incompatible BC$_3$-1S$_1$-6 individual have proven to be valuable resources. Furthermore, the seeds from the SC-Chiifu Lines described in this study will be made accessible to researchers for further functional genomics studies, thereby facilitating broader exploration and utilization of these valuable genetic resources.

B. rapa typically exhibits SI, overcoming this trait is not only crucial for utilizing the Chiifu line but also plays a pivotal role in enhancing *B. rapa* hybrid seed production using self-compatible lines within the male-sterile system. The conversion of male parental lines and maintainer lines into self-compatible lines is essential for the hybrid seed production process. Self-compatible lines streamline the reproduction process through honeybee pollination and circumvent crossing incompatibility during hybrid seed production. The G1277C mutation within *MLPK* represents a rare mutation. Among 841 accessions of *B. rapa* analyzed, only a minority, specifically eight accessions, exhibited the G1277C mutation. Assessment of CI values revealed that these eight accessions all demonstrated SC. In response to the G1277C, we developed a self-compatibility-specific marker, SC-MLPK. Following experimental optimization, this marker exhibited
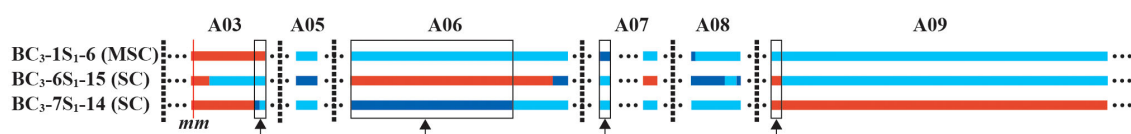

FIGURE 5
Identification of the shared segments in BC$_3$-6S$_1$-15 and BC$_3$-7S$_1$-14 but not in BC$_3$-1S$_1$-6. Light blue segments indicated the homozygous genotype identical to Chiifu; navy blue segments indicate the heterozygous genotype; red segments indicate the homozygous R-o-18 genotype. Arrows indicate the shared segments between BC$_3$-6S$_1$-15 and BC$_3$-7S$_1$-14.

stable and accurate genotyping characteristics, making it widely applicable for the creation of self-compatible *B. rapa* lines. The successful utilization of SC-MLPK for overcoming SI serves as a valuable reference for the cultivation of self-compatible *B. rapa* lines.

The success of MABC critically depends on the development of molecular markers that are not only evenly distributed, operationally straightforward, and cost-effective but also high in density for precise genetic background analysis. HRM genotyping technology offers distinct advantages in meeting these criteria. In a previous study, we developed 148 HRM markers evenly distributed in the genome based on a physical map to differentiate between four heading and four non-heading *B. rapa* (Chen et al., 2021). In this study, we expanded upon this approach by developing 131 HRM markers evenly distributed across the *B. rapa* genome, guided by both physical and genetic maps, to differentiate between Chinese cabbage line Chiifu and yellow sarson line R-o-18. These 279 HRM markers represent a powerful tool in *B. rapa* genetics and breeding.

Notably we observed segregation in SI and SC among plants with *mm* genotypes in the both BC_2S_1 and BC_3S_1 generations. This is different from the observation in germplasm screening that all the eight accessions with G1277C mutation were SC. These observations suggested the potential for overcoming SI barriers or reinforcing SC through the incorporation of gene(s) beyond *MLPK*. Put differently, under a genetic background akin to Chiifu, individuals carrying solely *mm* genotypes prove inadequate in overcoming its self-incompatibility. To obtain self-compatible Chiifu lines, it is imperative to consider not only the *MLPK* locus but also other loci influencing self-compatibility. This necessity compromises our ability to achieve a PR of 100% in obtaining the SC-Chiifu Lines. Through the identification of boundaries of the three selected individuals in the BC_3S_1 generation, we detected four candidate segments potentially regulating SI. Additionally, lines SC-Chiifu-a and SC-Chiifu-b (CI > 7) overcame SI and reached SC levels, albeit not reaching the SC level of R-o-18 (CI = 12). This suggested that besides the gene(s) in the four candidate segments, *S* haplotype and *MLPK*, other gene(s) may influence SC. Further exploration through the construction of genetic populations can elucidate the genetic mechanisms involved in overcoming SI barriers or enhancing SC. Such investigations hold promise for advancing our understanding of SC mechanisms in *Brassica* and for developing more efficient breeding strategies.

Data availability statement

The datasets presented in this study can be found in online repositories. The names of the repository/repositories and accession number(s) can be found in the article/Supplementary Material.

Author contributions

LC: Data curation, Formal analysis, Investigation, Methodology, Resources, Software, Writing – original draft, Writing – review & editing. JL: Resources, Writing – review & editing. XC: Formal analysis, Writing – review & editing. LZ: Resources, Writing – review & editing. YL: Methodology, Writing – review & editing. JW: Funding acquisition, Project administration, Writing – review & editing. XW: Funding acquisition, Project administration, Resources, Supervision, Writing – review & editing.

Funding

Conflict of interest

The authors declare that the research was conducted in the absence of any commercial or financial relationships that could be construed as a potential conflict of interest.

Publisher's note

All claims expressed in this article are solely those of the authors and do not necessarily represent those of their affiliated organizations, or those of the publisher, the editors and the reviewers. Any product that may be evaluated in this article, or claim that may be made by its manufacturer, is not guaranteed or endorsed by the publisher.

Supplementary material

The Supplementary Material for this article can be found online at: https://www.frontiersin.org/articles/10.3389/fpls.2024.1397018/full#supplementary-material

References

Breslauer, K. J., Frank, R., Blöcker, H., and Marky, L. A. (1986). Predicting DNA duplex stability from the base sequence. *Proc. Natl. Acad. Sci. U.S.A.* 83, 3746–3750. doi: 10.1073/pnas.83.11.3746

Cabrillac, D., Cock, J. M., Dumas, C., and Gaude, T. (2001). The S-locus receptor kinase is inhibited by thioredoxins and activated by pollen coat proteins. *Nature* 410, 220–223. doi: 10.1038/35065626

Cai, C., Wang, X., Liu, B., Wu, J., Liang, J., Cui, Y., et al. (2017). Brassica rapa Genome 2.0: A Reference Upgrade through Sequence Re-assembly and Gene Re-annotation. *Mol. Plant* 10, 649–651. doi: 10.1016/j.molp.2016.11.008

Cai, X., Chang, L., Zhang, T., Chen, H., Zhang, L., Lin, R., et al. (2021). Impacts of allopolyploidization and structural variation on intraspecific diversification in Brassica rapa. *Genome Biol.* 22, 166. doi: 10.1186/s13059-021-02383-2

Cai, X., Wu, J., and Wang, X. (2023). Harvesting knowledge: illuminating advances in Brassica crops genomics and breeding. *Horticulturae* 9, 1332. doi: 10.3390/horticulturae9121332

Chang, L., Liang, J., Zhang, L., Zhang, Z., Cai, X., Wu, J., et al. (2023). A complex locus regulates highly lobed-leaf formation in Brassica juncea. *Theor. Appl. Genet.* 136, 224. doi: 10.1007/s00122-023-04473-0

Chen, R., Chang, L., Cai, X., Wu, J., Liang, J., Lin, R., et al. (2021). Development of inDel markers for Brassica rapa based on a high-resolution melting curve. *Hortic. Plant J.* 7, 31–37. doi: 10.1016/j.hpj.2020.05.003

Chen, S., Zhou, Y., Chen, Y., and Gu, J. (2018). fastp: an ultra-fast all-in-one FASTQ preprocessor. *Bioinformatics* 34, i884–i890. doi: 10.1093/bioinformatics/bty560

Cheng, F., Wu, J., Cai, C., Fu, L., Liang, J., Borm, T., et al. (2016). Genome resequencing and comparative variome analysis in a Brassica rapa and Brassica oleracea collection. *Sci. Data* 3, 160119. doi: 10.1038/sdata.2016.119

Distefano, G., Caruso, M., La Malfa, S., Gentile, A., and Wu, S. B. (2012). High resolution melting analysis is a more sensitive and effective alternative to gel-based platforms in analysis of SSR–an example in citrus. *PLoS One* 7, e44202. doi: 10.1371/journal.pone.0044202

Dou, J., Wang, Y., Yang, H., Niu, H., Liu, D., Yang, S., et al. (2022). Development of branchless watermelon near isogenic lines by marker assisted selection. *Hortic. Plant J.* 8, 627–636. doi: 10.1016/j.hpj.2022.07.003

Herrmann, M. G., Durtschi, J. D., Wittwer, C. T., and Voelkerding, K. V. (2007). Expanded instrument comparison of amplicon DNA melting analysis for mutation scanning and genotyping. *Clin. Chem.* 53, 1544–1548. doi: 10.1373/clinchem.2007.088120

Jung, H. J., Jung, H. J., Ahmed, N. U., Park, J. I., Kang, K. K., Hur, Y., et al. (2012). Development of self-compatible B. rapa by RNAi-mediated S locus gene silencing. *PLoS One* 7, e49497. doi: 10.1371/journal.pone.0049497

Kakita, M., Murase, K., Iwano, M., Matsumoto, T., Watanabe, M., Shiba, H., et al. (2007). Two distinct forms of M-locus protein kinase localize to the plasma membrane and interact directly with S-locus receptor kinase to transduce self-incompatibility signaling in Brassica rapa. *Plant Cell* 19, 3961–3973. doi: 10.1105/tpc.106.049999

Li, H., and Durbin, R. (2009). Fast and accurate short read alignment with Burrows-Wheeler transform. *Bioinformatics* 25, 1754–1760. doi: 10.1093/bioinformatics/btp324

Li, H., Gu, A., Feng, D., Li, N., Yang, R., Zhang, X., et al. (2023). Fast tracking alien gene discovery by molecular markers in a late flowering Chinese cabbage-cabbage translocation line 'AT7–4'. *Hortic. Plant J.* 9, 89–97. doi: 10.1016/j.hpj.2021.11.009

Li, H., Handsaker, B., Wysoker, A., Fennell, T., Ruan, J., Homer, N., et al. (2009). The sequence alignment/map format and SAMtools. *Bioinformatics* 25, 2078–2079. doi: 10.1093/bioinformatics/btp352

Liu, X., Dong, S., Miao, H., Bo, K., Li, C., Yang, Y., et al. (2022). Genome-wide analysis of expansins and their role in fruit spine development in cucumber (Cucumis sativus L.). *Hortic. Plant J.* 8, 757–768. doi: 10.1016/j.hpj.2021.11.004

Liu, J., Liu, B., Cheng, F., Liang, J., Wang, X., and Wu, J. (2016). A high density linkage map facilitates QTL mapping of flowering time in Brassica rapa. *Hortic. Plant J.* 2, 217–223. doi: 10.1016/j.hpj.2016.11.003

Mavrodiev, E. V., Dervinis, C., Whitten, W. M., Gitzendanner, M. A., Kirst, M., Kim, S., et al. (2021). A new, simple, highly scalable, and efficient protocol for genomic DNA extraction from diverse plant taxa. *Appl. Plant Sci.* 9, e11413. doi: 10.1002/aps3.11413

McKenna, A., Hanna, M., Banks, E., Sivachenko, A., Cibulskis, K., Kernytsky, A., et al. (2010). The Genome Analysis Toolkit: a MapReduce framework for analyzing next-generation DNA sequencing data. *Genome Res.* 20, 1297–1303. doi: 10.1101/gr.107524.110

Murase, K., Shiba, H., Iwano, M., Che, F. S., Watanabe, M., Isogai, A., et al. (2004). A membrane-anchored protein kinase involved in Brassica self-incompatibility signaling. *Science* 303, 1516–1519. doi: 10.1126/science.1093586

Nasrallah, J. B., and Nasrallah, M. E. (1993). Pollen[mdash]Stigma signaling in the sporophytic self-incompatibility response. *Plant Cell* 5, 1325–1335. doi: 10.2307/3869785

Ohata, M., Takada, Y., Sato, Y., Okamoto, T., Murase, K., Takayama, S., et al. (2023). MLPK function is not required for self-incompatibility in the S29 haplotype of Brassica rapa L. *Plant Reprod.* 36, 255–262. doi: 10.1007/s00497-023-00463-w

Oikawa, E., Takuno, S., Izumita, A., Sakamoto, K., Hanzawa, H., Kitashiba, H., et al. (2011). Simple and efficient methods for S genotyping and S screening in genus Brassica by dot-blot analysis. *Mol. Breed.* 28, 1–12. doi: 10.1007/s11032-010-9455-8

Robinson, J. T., Thorvaldsdóttir, H., Winckler, W., Guttman, M., Lander, E. S., Getz, G., et al. (2011). Integrative genomics viewer. *Nat. Biotechnol.* 29, 24–26. doi: 10.1038/nbt.1754

SantaLucia, J. Jr. (1998). A unified view of polymer, dumbbell, and oligonucleotide DNA nearest-neighbor thermodynamics. *Proc. Natl. Acad. Sci. U.S.A.* 95, 1460–1465. doi: 10.1073/pnas.95.4.1460

Stone, S. L., Arnoldo, M., and Goring, D. R. (1999). A breakdown of Brassica self-incompatibility in ARC1 antisense transgenic plants. *Science* 286, 1729–1731. doi: 10.1126/science.286.5445.1729

Untergasser, A., Cutcutache, I., Koressaar, T., Ye, J., Faircloth, B. C., Remm, M., et al. (2012). Primer3–new capabilities and interfaces. *Nucleic Acids Res.* 40, e115. doi: 10.1093/nar/gks596

Wang, X., Wang, H., Wang, J., Sun, R., Wu, J., Liu, S., et al. (2011). The genome of the mesopolyploid crop species Brassica rapa. *Nat. Genet.* 43, 1035–1039. doi: 10.1038/ng.919

White, H. E., Hall, V. J., and Cross, N. C. (2007). Methylation-sensitive high-resolution melting-curve analysis of the SNRPN gene as a diagnostic screen for Prader-Willi and Angelman syndromes. *Clin. Chem.* 53, 1960–1962. doi: 10.1373/clinchem.2007.093351

Xiao, Z., Han, F., Hu, Y., Xue, Y., Fang, Z., Yang, L., et al. (2019). Overcoming cabbage crossing incompatibility by the development and application of self-compatibility-QTL- specific markers and genome-wide background analysis. *Front. Plant Sci.* 10. doi: 10.3389/fpls.2019.00189

Yamamoto, M., Ishii, T., Ogura, M., Akanuma, T., Zhu, X. Y., and Kitashiba, H. (2023). S haplotype collection in Brassicaceae crops-an updated list of S haplotypes. *Breed Sci.* 73, 132–145. doi: 10.1270/jsbbs.22091

Zhang, L., Cai, X., Wu, J., Liu, M., Grob, S., Cheng, F., et al. (2018). Improved Brassica rapa reference genome by single-molecule sequencing and chromosome conformation capture technologies. *Hortic. Res.* 5, 50. doi: 10.1038/s41438-018-0071-9

Zhang, Z., Guo, J., Cai, X., Li, Y., Xi, X., Lin, R., et al. (2022b). Improved reference genome annotation of Brassica rapa by pacific biosciences RNA sequencing. *Front. Plant Sci.* 13. doi: 10.3389/fpls.2022.841618

Zhang, L., Huang, J., Su, S., Wei, X., Yang, L., Zhao, H., et al. (2021). FERONIA receptor kinase-regulated reactive oxygen species mediate self-incompatibility in Brassica rapa. *Curr. Biol.* 31, 3004–3016.e3004. doi: 10.1016/j.cub.2021.04.060

Zhang, L., Li, X., Chang, L., Wang, T., Liang, J., Lin, R., et al. (2022a). Expanding the genetic variation of Brassica juncea by introgression of the Brassica rapa Genome. *Hortic. Res.* 9. doi: 10.1093/hr/uhab054

Zhang, L., Liang, J., Chen, H., Zhang, Z., Wu, J., and Wang, X. (2023). A near-complete genome assembly of Brassica rapa provides new insights into the evolution of centromeres. *Plant Biotechnol. J.* 21, 1022–1032. doi: 10.1111/pbi.14015

Zheng, J., Zhao, H., Ma, Y., Jiang, M., Zhan, Z., Li, X., et al. (2022). Marker-Assisted Pyramiding of Genes for Multilocular Ovaries, Self-Compatibility, and Clubroot Resistance in Chinese Cabbage (Brassica rapa L. ssp. pekinensis). *Horticulturae* 8, 139. doi: 10.3390/horticulturae8020139